[Supplementary material]

Holocene resource exploitation along the Nile: diet and subsistence strategies of Mesolithic and Neolithic societies at Khor Shambat 1, Sudan

Julie Dunne[1,*], Maciej Jórdeczka[2], Marek Chłodnicki[3], Karen Hardy[4,5], Lucy Kubiak-Martens[6], Magdalena Moskal-del Hoyo[7], Marta Osypińska[8], Marta Portillo[9], Iwona Sobkowiak-Tabaka[10], Selina Delgado-Raack[5], Przemysław Bobrowski[2], Paul S. Breeze[11], Nick Drake[11,12], Katie Manning[11] & Richard P. Evershed[1]

[1] Organic Geochemistry Unit, School of Chemistry, University of Bristol, UK

[2] Institute of Archaeology and Ethnology, PAS, Poznań, Poland

[3] Archaeological Museum in Poznań, Poland

[4] Catalan Institution for Research and Advanced Studies (ICREA), Barcelona, Spain

[5] Departament de Prehistòria, Facultat de Filosofia i Lletres, Universitat Autònoma de Barcelona, Spain

[6] BIAX Consult, Biological Archaeology & Environmental Reconstruction, Zaandam, the Netherlands

[7] W. Szafer Institute of Botany PAS, Krakow, Poland

[8] Institute of Archaeology, University of Wrocław, Poland

[9] Department of Archaeology and Anthropology, Institució Milà i Fontanals, Spanish National Research Council (IMF-CSIC), Barcelona, Spain

[10] Faculty of Archaeology, Adam Mickiewicz University, Poznan, Poland

[11] Department of Geography, King's College London, UK

[12] The Max Planck Institute for the Science of Human History, Jena, Germany

[*]Author for correspondence ✉ julie.dunne@bristol.ac.uk

Table S1. Lab number, phase, sample number, site location, vessel form, decoration, lipid concentration (μg g^{-1}), $\delta^{13}C$ and $\Delta^{13}C$ values and attributions of KSH1 potsherds.

Laboratory Number	Phase	Sample no.	Depth/location	Vessel form	Decoration	Lipid concentration (μg g^{-1})	$\delta^{13}C_{16:0}$	$\delta^{13}C_{18:0}$	$\Delta^{13}C$	Attribution
KSH002	Neolithic	9	Trench 2, layer 1 (0–0.1m)	Not known	I.B Impressed ware-dotted zigzag	113.9	−20.2	−22.3	−2.1	Ruminant adipose
KSH003	Neolithic	14	Trench 2, layer 3 (0.2–0.3m)	Not known	I.C (RSI) Impressed ware-lines of dots and vees	285.4	−20.1	−18.7	1.4	Non ruminant/plant
KSH005	Neolithic	17	Trench 2, layer 4 (0.3–0.4m)	Not known	IV.D (INS3) Incised ware-horizontal lines	26.0	−23.7	−24.9	−1.3	Ruminant adipose
KSH008	Neolithic	6	Trench 1, layer 1 (0–0.1m)	Not known	Undecorated (Plain ware)	146.7	−24.4	−26.4	−2.0	Ruminant adipose
KSH1953	Neolithic	38	Trench 5	Not known	I.B dotted zigzag	22.2	−14.1	−15.7	−1.6	Ruminant adipose
KSH1956	Neolithic	132	Trench 5, layer 1	Simple closed form	undecorated	24.0	−20.7	−18.7	1.9	Non ruminant/plant
KSH1958	Neolithic	149	Trench 2, layer 4	Not known	Black top	196.0	−23.5	−26.1	−2.6	Ruminant adipose
KSH1959	Neolithic	195	Trench 5, layer 3	Simple closed form	I.B dotted zigzag	6.4	−21.5	−25.3	−3.8	Ruminant dairy
KSH1962	Neolithic	250	Surface	Not known	IV.D semi−circular panels of incised line	32.8	−19.2	−21.6	−2.4	Ruminant adipose
KSH1964	Neolithic	308	Trench 5	Not known	I.B dotted zigzag	43.1	−24.8	−27.5	−2.6	Ruminant adipose
KSH1965	Neolithic	342	Trench 1, surface	Not known	I.B dotted zigzag	173.9	−23.9	−26.3	−2.3	Ruminant adipose
KSH1967	Neolithic	390	Trench 2, layer 3	Not known	I.B dotted zigzag	17.7	−19.6	−19.4	0.2	Ruminant/non−ruminant adipose

KSH1968	Neolithic	448	Trench 7, 0.8–1m	Not known	IV.D semicircular panels of incised line	49.1	−20.3	−22.5	−2.2	Ruminant adipose
KSH1977	Neolithic	765	Trench 6, m.162, 0.6–0.8m	Not known	I.B dotted zigzag	92.0	−21.4	−23.6	−2.2	Ruminant adipose
KSH1979	Neolithic	853	Prof. E, m.164, 1.3–1.4m	Not known	undecorated	13.7	−25.3	−27.8	−2.5	Ruminant adipose
KSH1981	Mesolithic	909	Trench 7, 1–1.1m	Not known	II.J3 dotted wavy−line	14.2	−19.8	−18.5	1.3	Non ruminant/plant
KSH1983	Neolithic	1031	Trench 5, layer 3	Not known	I.B dotted zigzag	7.0	−15.9	−14.2	1.8	Non ruminant/plant
KSH1991	Neolithic	1174	Trench 7, 0.6–0.8m	Simple closed form	IV.D semicircular panels of incised line	205.5	−23.0	−23.5	−0.5	Ruminant/non−ruminant adipose
KSH1994	Neolithic	1185	Grave 28, prof. E	Not known	IV.D semicircular panels of incised line	16.4	−24.2	−23.2	1.1	Non ruminant/plant
KSH1998	Neolithic	1505	Trench 2, layer 3	Not known	I.A plain zigzag	42.1	−19.1	−21.6	−2.5	Ruminant adipose
KSH1999	Mesolithic	1513	Trench 5, 0.4–0.6m, secondary deposit	Not known	II.J3 dotted wavy−line	15.2	−24.6	−23.2	1.4	Non ruminant/plant
KSH2009	Neolithic	1578	Trench 2, layer 2	Not known	I.A plain zigzag	11.3	−22.3	−21.6	0.6	Non ruminant/plant
KSH2011	Mesolithic	1580	Trench 2, layer 2	Simple open form	II.J3 dotted wavy−line	6.0	−24.4	−20.9	3.4	Non ruminant/plant
KSH2020	Mesolithic	2548	Trench 6, 1.4m	Not known	II.J3 dotted wavy−line	33.7	−19.0	−18.5	0.5	Non ruminant/plant
KSH2021	Mesolithic	2551	Trench 6, 1.3m, close to grave 28	Simple closed form	II.J3 dotted wavy−line	37.5	−18.8	−20.5	−1.7	Ruminant adipose
KSH2025	Mesolithic	2560	Trench 6, 1.4–1.4m	Simple closed form	II.J3 dotted wavy−line	16.1	−22.3	−21.6	0.6	Non ruminant/plant
KSH2026	Mesolithic	2561	Trench 6, 1.2–1.3m	Simple open form	II.J3 dotted wavy−line	10.2	−21.4	−20.9	0.5	Non ruminant/plant
KSH2028	Mesolithic	2569	Trench 6, 1.30–1.4m	Not known	II.J3 dotted wavy−line	42.4	−22.9	−22.4	0.5	Non ruminant/plant

KSH2033	Mesolithic	2594	Trench 6, feature 16	Not known	IB.Bw wavy line	106.2	−18.8	−18.3	0.5	Non ruminant/plant
KSH2035	Mesolithic	2598	Trench 9, m. 215–220, Profile E	Unknown; perforation for handling under the rim	I.B dotted zigzag	133.8	–	–	–	Plant
KSH2173	Neolithic	140	Trench 4, 0.2–0.4m	Simple closed form	undecorated	10.6	−16.0	−17.8	−1.8	Ruminant adipose

1. Archaeobotanical analysis: material and methods

Systematic sampling for archaeobotanical analysis resulted in the collection of 116 samples during the 2016, 2017 and 2018 campaigns (Table S2). Samples were taken from various contexts, including settlement units (Features 1, 2 and 3), hearths, graves, and from a pot deposited in one of the graves. Archaeobotanical samples were collected within a 1 × 1m grid, which was vertically subdivided into 0.10m−thick layers. The soil sample sizes ranged from approximately 250ml to 4.5 litres, depending on the size of the excavated deposit. Dry sieving was found to be the appropriate recovery technique and all samples were dry sieved through 1.0mm and 0.5mm sieves in the field laboratory. Plant remains were sorted and briefly identified. During the sorting process, wood charcoal was collected separately for further botanical analysis.

Table S2. Khor Shambat, Sudan (KSH1, field seasons 2016 to 2018: plant macroremains and charcoal. Frequency scale: − = no plant remains other than charcoal; + = few fragments, ++ = numerous.

Chronology	Sample	Field season	Sample location	Level (cm)	Plant macroremains*	Charcoal	Bone	Fish
Early Mesolithic	−	2018	Trench 6, Feature 14	LF.120, L 260	−	Ziziphus sp. 6frg	.	.
Early Mesolithic	−	2018	Trench 6, Feature 14	LF.100−120, L. 240−260	−	Ziziphus sp. 1frg	.	.
Early Mesolithic	−	2018	Trench 6, Feature 14	SE part LF.100, L. 240	−	indet.+	.	.
Late Mesolithic	−	2018	Trench 6, Feature 14	LF 3−5 (F.14. p.E) L 140−150	−	indet.+	.	.
Mesolithic	B1	2017	square 165/55	120−130	−	Ziziphus sp. 7frg	.	.
Mesolithic	B2	2017	square 165/56, Pit10	120−130	−	Ziziphus sp. 4frg	.	.
Mesolithic	B3	2017	square165/56	120−130	−	Ziziphus sp. 10frg	+	.
Mesolithic	B10	2017	square 164/55	100−110	−	Ziziphus sp. 1frg	+	.
Mesolithic	B14	2017	square165/56	80	*Ziziphus spina-christi*, fruit stone 6frg	Acacia sp. 4frg, Ziziphus sp. 4frg, indet. broad-leaved 7frg	+	+
Mesolithic	B15	2017	square 167/55	80−90	*Ziziphus spina-christi*, fruit stone 2frg	Ziziphus sp. 4frg, indet. broad−leaved 1frg, indet.+	.	.
Mesolithic	B16	2017	square 162/55	95−100	−	Ziziphus sp. 8frg	.	.
Mesolithic	B17	2017	square 165/55	35	−	Ziziphus sp. 2frg	.	.
Mesolithic	B25	2017	Profile 164/56	120−130	−	indet.++	+	.
Mesolithic	B28	2017	square 166/56	100−110	−	indet.+	.	.
Mesolithic	B29	2017	square 166/56	100−110	−	indet.+	+	+
Mesolithic	B30	2017	square 167/56	130	−	indet.+	.	.
Mesolithic	B31	2017	square 167/56	90−100	−	*no charcoal*	+	+
Mesolithic	B32	2017	square 164/56	110	−	Ziziphus sp. 2frg, indet. Broad-leaved 1frg	+	.
Mesolithic	B33	2017	fire place	95−100	*Ziziphus spina-christi*, fruit stone 1frg	Grewia sp. 4frg, Ziziphus sp. 2frg, indet. broad-leaved 4frg, indet.+	+	+
Mesolithic	B34	2017	square 165/55	100−110	−	Ziziphus sp. 1frg, indet. Broad-leaved 1frg	+	.
Mesolithic	B35	2017	Profile 164/56	120−130	−	Ziziphus sp. 10frg, indet.+	.	.
Mesolithic	B36	2017	square165/56, Pit10	130−140	−	Ziziphus sp. 5frg	.	.

Mesolithic	B38	2017	Grave47	.	–	Acacia sp. 3frg, indet.+	.	.
Mesolithic	B40	2017	Grave 47	.	–	Ziziphus sp. 10frg, indet.+	.	.
Mesolithic	B41	2017	Pit10	.	–	Ziziphus sp. 5frg, indet.+	.	.
Mesolithic	B42	2017	Grave 47 near the head	.	–	Ziziphus sp. 1frg	.	.
Mesolithic	B39	2017	square 165/56, Pit10	130	–	Ziziphus sp. 5frg, indet.+	.	.
Mesolithic/Neolithic	B26	2017	square 165/56	85	–	indet.+	.	.
Neolithic	B5	2017	Grave 46	.	–	indet.+	+	.
Neolithic	B7	2017	square 168	55	–	indet.+	+	.
Neolithic	B11	2017	square 166/56	70–80	–	indet.+	.	.
Neolithic	B12	2017	square 166/56	70–80	indet. nut shell 3frg	Acacia sp. 2frg, Ziziphus sp. 4frg, indet. broad-leaved 6frg	+	+
Neolithic	B13	2017	square 165/5	20	–	indet.+	.	.
Neolithic	B18	2017	square 163	70	–	indet.+	.	.
Neolithic	B19	2017	square 167/56	70	–	Acacia sp. 1frg	+	+
Neolithic	B20	2017	square 166/55	85	–	Acacia sp. 4frg, Ziziphus sp. 6frg	.	.
Neolithic	B21	2017	square 166	65–70	–	Acacia sp. 3frg, indet.+	.	.
Neolithic	B22	2017	square 166/56, Grave46	60–70	–	Acacia sp. 10frg, Ziziphus sp. 1frg, indet. broad-leaved 2frg	.	.
Neolithic	B23	2017	square 166	65–70	–	indet.+	.	.
Neolithic	B24	2017	square 166/55	60–70	–	Acacia sp. 5frg, indet.+	.	.
Neolithic	–	2018	Trench 6, Grave 51	pot 3	–	Acacia sp. 4frg, indet. broad-leaved 1frg	.	.
Neolithic	–	2018	Trench 6, Grave 51	grave filling	–	indet.+	.	.
Neolithic	4	2016	Feature 1 (ashy filling), profile 164cm	80–100	*Ziziphus spina-christi*, fruit stone 4 frg; *Celtis integrifolia*, fruit stone 5frg	indet.++	.	+
Neolithic	5	2016	Grave 15	–	*Zizyphus* cf. spina-christi, fruit stone 1frg	indet.+	.	.
Neolithic	6	2016	Profile 1, Feature 1	140 (bottom part, near the grave)	*Ziziphus spina-christi*, fruit stone 1frg	Acacia sp. 2frg, cf. *Balanites aegyptiaca* 2frg, Ziziphus sp. 5frg, indet. broad-leaved 1frg	.	.
Neolithic	7	2016	Profile 161cm	80	*Ziziphus spina-christi*, fruit stone 1frg	indet.+	.	.
Neolithic	9	2016	Profile, Feature 1	60–80	*Ziziphus spina-christi*, fruit stone 12 frg; *Celtis integrifolia*, fruit stone 6frg	Acacia sp. 1frg, cf. *Capparis decidua* 8frg, Ziziphus sp. 1frg	.	++

Neolithic	10	2016	Profile, Feature 1	140	Ziziphus spina−christi, fruit stone 6frg; Celtis integrifolia, fruit stone 4frg	Ziziphus sp. 10frg	.	+
Neolithic	25	2016	Trench 6, Feature 1	50−60	Ziziphus spina−christi, fruit stone 1x+ 4frgs; Celtis integrifolia, fruit stone 7frg	indet.+	.	+
Neolithic	26	2016	Trench 6, Feature 1	60−70	Celtis integrifolia, fruit stone 5frg	indet.+	.	+
Neolithic	27	2016	Trench 6, Feature 1	40−50	Celtis integrifolia, fruit stone 8frg	indet.+	.	+
Neolithic	29	2016	Trench 6, Feature 1	50−60	Celtis integrifolia, fruit stone+++	indet.+	.	+
Neolithic	32	2016	Trench 6, Feature 1	70−80	Ziziphus spina−christi, fruit stone 5frg	indet.+	.	.
Neolithic	37	2016	Trench 6, Feature 1	70	−	indet.++	.	.
Neolithic	38	2016	Trench 6, Feature 1	70−90	Ziziphus spina−christi, fruit stone 5frg; Celtis integrifolia, fruit stone 3frg	indet.++	.	.
Neolithic	40	2016	Trench 6, Feature 2	80−100	−	Ziziphus sp. 9frg	.	.
Neolithic	41	2016	Trench 6, Feature 3	70	−	Acacia sp. 3frg, Ziziphus sp. 1frg	.	++
Neolithic	42	2016	Trench 6, Feature 1	70	−	Acacia sp. 14frg, cf. *Capparis decidua* 1frg	.	.
Neolithic	43	2016	Profiel W, Feature 1 (layer with ash)		Celtis integrifolia, fruit stone 9frg	indet.+	.	+
Neolithic	45	2016	Trench 6, Feature 1	70−80	−	Acacia sp. 5frg	.	.
Neolithic	46	2016	Trench 6, Feature 1	70−80	Ziziphus spina−christi, fruit stone 4frg	Acacia sp. 8frg, Ziziphus sp. 2frg, indet. broad-leaved 2frg	.	.
Neolithic	52	2016	Trench 6, Feature 3	80−90	−	indet.++	.	.
Neolithic	53	2016	Trench 6, Feature 1	90−100	Ziziphus spina−christi, fruit stone 3frg; Celtis integrifolia, fruit stone 5frg	Ziziphus sp. 3frg	.	.
Neolithic	54	2016	Trench 6, Feature 3	70−80	Ziziphus spina−christi, fruit stone 3frg; Celtis integrifolia, fruit stone 7frg	Acacia sp. 6frg, cf. *Balanites aegyptiaca* 1frg, Ziziphus sp. 4frg, indet. broad-leaved 1frg	.	.
Neolithic	56	2016	Trench 6, Feature 3	80−90	−	Ziziphus sp. 1frg	.	.
Neolithic	62	2016	Trench 6, Feature 1	120−140	Ziziphus spina−christi, fruit stone 7frg; Celtis integrifolia, fruit stone 3frg	indet.++	.	+
Neolithic?	16	2016	Trench 7	110−120	Ziziphus spina−christi, fruit stone 2frg	indet.+	.	+
Neolithic?	B8	2017	Grave 39 (fill)	.	Celtis integrifolia, fruit stone 3x + 28frg	*no charcoal*	.	.

* The fruit stones of Ziziphus are all charred; fruit stones of Celtis are heavily silicified, and can survive in archaeological deposits in desiccated form.

Plant macro−remains were identified botanically at the BIAX *Consult* laboratory in The Netherlands with the use of the Leica binocular incident light microscope at a magnification of 6× to 50×. Unfortunately, the diversity of plant species was relatively low, and the plant remains assemblages were dominated by charcoal remains. Aside from charcoal, the only plant remains comprised charred fragments of fruit stones of *Ziziphus* (most likely *Ziziphus spina−christi*; Figure 3), also found at other early and middle Holocene sites in Central and Northern Sudan, and in Southern Egypt (cf. Majid 1989; Kubiak−Martens 2011; Beldados 2015, 2017 and African hackberry (*Celtis integrifolia*; Figure 3). There are several possible explanations for this limited preservation of plant remains. The degree of fragmentation of the charcoal remains suggests significant erosion (most likely from wind) and exposure to alternating wet and dry conditions after the site was abandoned.

Charcoal remains (Tables S3 & S4) were analysed at the Department of Palaeobotany of the W. Szafer Institute of Botany of the Polish Academy of Sciences (IB PAS). For anthracological analysis, a reflected light microscope with magnifications of 100×, 200× and 500× (Zeiss Axio) was used to observe the wood anatomy in three anatomical sections of the wood: transverse section, longitudinal radial section and longitudinal tangential section in freshly broken charcoal fragments. Taxonomical identifications were made by comparing the specimens with the modern wood collections of the IB PAS and the Atlas on Wood Anatomy (Neumann *et al.* 2001). The botanical determinations were made in consultation with Dr. Alexa Höhn. Dendrological analysis focused on ring curvature observations were performed (Marguerie & Hunot 2007) and revealed an occurrence of various fragments coming from twigs and branch wood (Tables S3 & S4). The presence of fungi preserved inside vessels and other elements of wood anatomy was noted (Tables S2 & S4; Figure S1C, H), which suggest the use of decayed wood as fuel (Moskal−del Hoyo *et al.* 2010)

Table S3. Mesolithic charcoal assemblages from Khor Shambat.

Khor Shambat, Mesolithic	**Sample number**															**Grave 47**			**Fireplace**
No. of samples	**B1**	**B2**	**B3**	**B10**	**B14**	**B15**	**B16**	**B17**	**B32**	**B34**	**B35**	**B36**	**B39**	**B41**	**Tr6, F14**	**B38**	**B40**	**B42**	**B33**
Acacia sp.					4											3			
Grewia sp.																			4
Ziziphus sp.	7	4	10	1	4	4	8	2	2	1	10	5	5	5	7		10	1	2
Broad-leaved					7	1			1	1									4
Sum of fragments	**7**	**4**	**10**	**1**	**15**	**5**	**8**	**2**	**3**	**2**	**10**	**5**	**5**	**5**	**7**	**3**	**10**	**1**	**10**
Twig																			1
Branch wood																			
Fungi		1	2		2		3				1				4	1			3

Table S4. Neolithic charcoal assemblages from Khor Shambat.

Khor Shambat, Neolithic	**Features**																	**Graves**	
No. of samples	**6**	**9**	**10**	**40**	**41**	**42**	**45**	**46**	**52**	**53**	**54**	**56**	**B12**	**B19**	**B20**	**B21**	**B24**	**B22, Grave 46**	**Grave 51**
Balanites aegyptiaca	2																		
Acacia sp.	2	1			3	14	5	8			6		2	1	4	3	5	10	4
Ziziphus sp.	5	1	10	9	1			2		3	4	1	4		6			1	2
cf. *Leguminosae-Papilionoideae*		8				1					1								
Broad-leaved	1							2			1		6					2	1
Sum of fragments	**10**	**10**	**10**	**9**	**4**	**15**	**5**	**12**	**0**	**3**	**12**	**1**	**12**	**1**	**10**	**3**	**5**	**13**	**7**
Twig													3						
Branch wood			2													2			

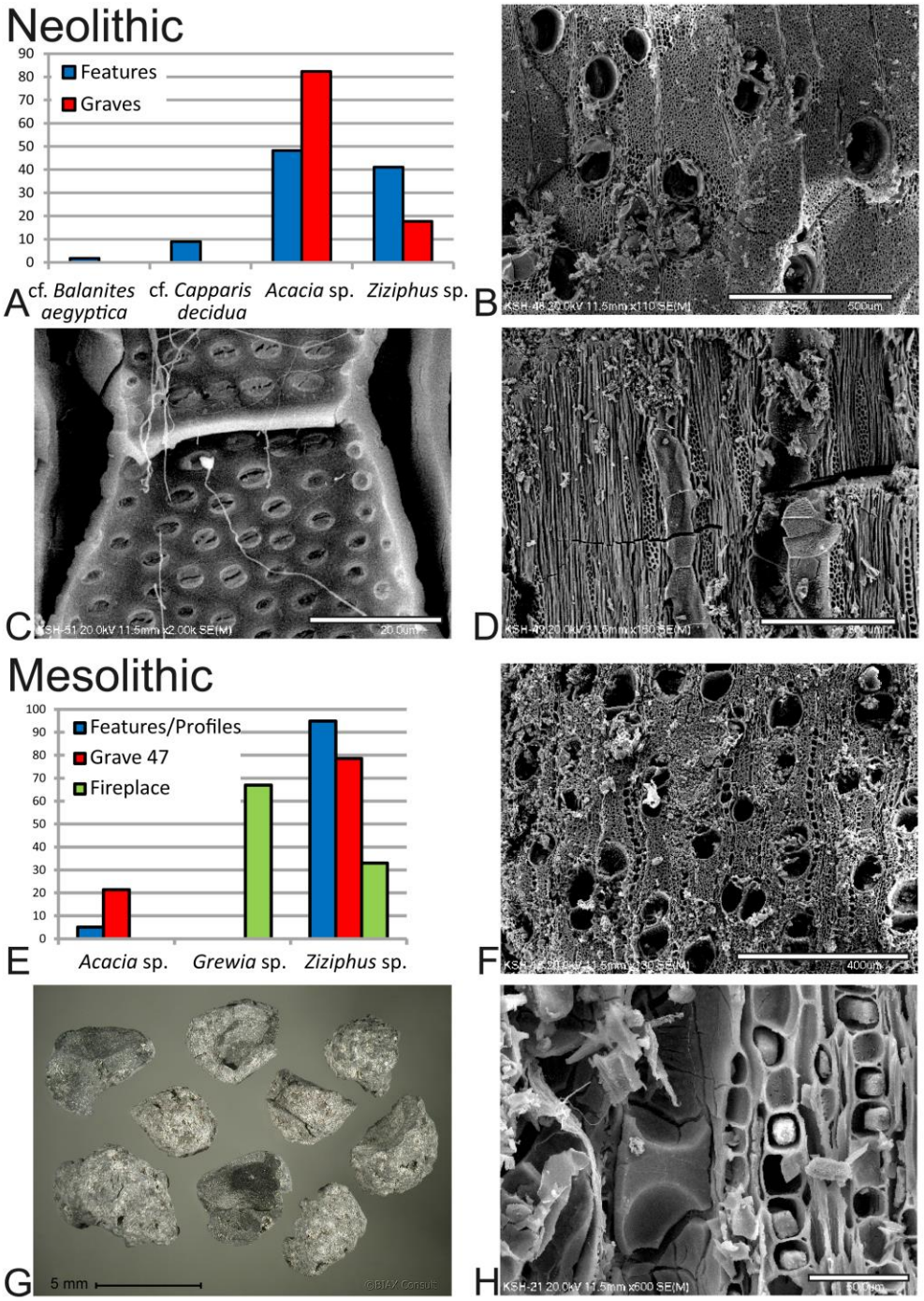

Figure S1. The main taxa found in the Neolithic and Mesolithic plant macro−remains assemblages from Khor Shambat: A–F, H) wood charcoals and G) charred fruit stones of Ziziphus spina−christi. *A) the relative frequency of taxa from the Neolithic charcoal assemblages; B)* Acacia *sp. in transverse section (TS); C) details of* Acacia *sp. in radial longitudinal section (RLS), with vestured pits in the vessels and hyphae of fungi; D)* Acacia *sp. in tangential longitudinal section (TLS); E) the relative frequency of taxa from the Mesolithic charcoal assemblages; F)* Ziziphus *sp. in TS; H)* Ziziphus *sp. in TLS, with crystals inside the rays and fungal hyphae. Scale bars: B) 500µm; C) 20µm; D) 300µm; F)*

400µm; H) 50 µm (micrographs by M. Moskal−del Hoyo; photographs by L. Kubiak−Martens).

The documentation of charcoal fragments in the form of micrographs was prepared by using a scanning electron microscope (SEM Hitachi S−4700) at the Laboratory of Field Emission Scanning Electron Microscopy and Microanalysis at the Institute of Geological Sciences of the Jagiellonian University (Kraków, Poland), with the assistance of A. Łatkiewicz. *Ziziphus* sp. (Figure S1F) and *Acacia* sp. (Figure S1B, D) were the most frequently found taxa among charcoal assemblages (Figure S1A, E), with the former being dominant in the Mesolithic assemblage, while the latter reached the highest frequency in the Neolithic period (Tables S3 and S4). Other taxa were documented sporadically, for example, *Grewia* sp. appeared in the Mesolithic layers, whereas cf. *Balanites aegyptica* occurred in the Neolithic layers (Figure S1). It is very difficult to distinguish between numerous species of *Acacia* and that is why only identification is given to genus level. The same is true for a few species of *Ziziphus* and *Grewia* (Neumann *et al.* 2001). The source of the charcoal is most likely the intentional use of wood for fuel in domestic hearths or roasting pits, which may be inferred after the presence of decayed wood, small diameter of some of the charcoals and a documentation of various woody taxa. Only one sample from the Mesolithic period (Table S3) was associated directly with a fireplace, but it contained a few fragments of charcoals from two different taxa. Wood might have been brought to the site for other purposes such as the construction of buildings/huts or as a raw material for making tools, but later burned as fuel. The firewood may have originated from local vegetation gathered relatively close to the site.

2. Faunal analysis: materials and methods

The osteological material discussed here was subject to analysis aimed at producing the most comprehensive taxonomic and anatomical identification of the remains possible. The analysis comprised several stages. In cases when there were well−preserved diagnostic features, the bones were identified according to taxa and anatomy based on comparable collections and relevant publications (Tables S5–S7; Walker 1985; Peters 1986, 1989a, 1989b; Van Neer 1989, 2009; Peters *et al.* 1997; Plug 2014). Remains completely devoid of diagnostic features were counted and recorded in terms of size class and grouped according to relevant contexts. Skeletal remains were also subject to verification and reassessment based on modern comparative collections in Belgium (L'Institut Royal des Sciences Naturelles de Belgique,

Palaeontological Research Unit, Ghent University). The anatomical origin of a given bone fragment along with the approximate age of the animal, sex and bone metric data were also noted.

Table S5. Mesolithic faunal remains by size.

Size class		Approximate weight (kg)	Examples	N / %
I	Small	2.7–10	Dik−dik, duiker, porcupine	92 / 17.62
II	Small–medium	10–70	Warthog, bushbuck, bohor	47 / 9.00
III	Large–medium	45–270	Waterbuck, bushpig,	262 / 50.19
IV	Large	300–950	Buffalo, giraffe, kudu	111 / 21.26
V	Mega−fauna	>950	Hippopotamus, rhinoceros	10 / 1.91

Table S6. Neolithic proportions: vertebrate remains/bones (fish, reptiles, birds without shells, mammals).

	N	%
DOMESTIC ANIMALS	454	43.90
WILD ANIMALS	580	56.10
TOTAL	**1 034**	**100**

Table S7. Neolithic proportions: mammals.

	N	%
DOMESTIC MAMMALS	454	66.86
GAME MAMMALS	225	33.14
TOTAL	**679**	**100**

Species distribution of the Khor Shambat remains was considered in several aspects: a general list of species registered at Early and Middle Holocene sites, the frequency and percentage shares of remains recorded in stratigraphic sediments at site as well as the frequency of individual species in particular excavation areas at Khor Shambat.
Given their largest frequency at Khor Shambat, the remains of domestic cattle were also analysed in terms of anatomical variation at individual locations. Due to the quantity of the data, the percentage of remains of morphologically immature individuals were also calculated. An osteometrical examination was carried out using standard measurements (Von Den Driesch 1976). Osteological materials from the excavated sites were subject to taphonomic observations. We analysed the state of preservation of the remains with respect to the location of their deposition, variability of natural conditions, the possibility of interpretation of the degree of their impact on the biostratinomic stage as well as identification possibilities.

3. Organic residue analysis: materials and methods

Lipid analysis and interpretations were performed using established protocols described in detail in earlier publications (Dudd & Evershed 1998; Correa−Ascencio & Evershed 2014). A total of 99 sherds were analysed, 39 from the Mesolithic and 60 from the Neolithic (Figures 5 & 6). The lipid recovery rate was good at 30 per cent overall, (*n*=30) although recovery was higher in the Neolithic (35 per cent, *n*=21) than the Mesolithic (22% per cent, *n*=9). The mean lipid concentration from the sherds was 0.06mg g^{-1}, with a maximum lipid concentration of 0.28mg g^{-1} (KSH003, Table S1). Analysis of the total lipid extracts (TLEs, *n*=100), using gas chromatography (GC) and gas chromatography−mass spectrometry (GC−MS), demonstrated that 30 sherds contained sufficient concentrations (>5μg g^{-1}) of lipids that can be reliably interpreted (Evershed 2008). These extracts comprised lipid profiles comprising free fatty acids, palmitic (C_{16}) and stearic (C_{18}), typical of a degraded animal fat (Figure 7a) (e.g. Evershed *et al.* 1997; Evershed *et al.* 2002). Significantly, lipid concentration for 73 per cent of the interpretable residues (*n*=22) was less than 50μg g^{-1}, with 50 per cent containing less than 30μg g^{-1} (*n*=15). Lipid concentrations are slightly lower in the Mesolithic than the Neolithic, which may reflect local preservation conditions or suggest these vessels were not used intensively.

All solvents used were HPLC grade (Rathburn) and the reagents were analytical grade (typically > 98% purity). An internal standard, typically 20 μg, was added to enable quantification of the lipid extract (*n*−tetratriacontane; Sigma Aldrich Company Ltd). Following the addition of 5mL of H_2SO_4/MeOH 2 − 4% ($\delta^{13}C$ measured), the culture tubes were placed on a heating block for 1h at 70°C, mixing every 10 min. Once cooled, the methanolic acid was transferred to test tubes and centrifuged at 2500 rpm for 10 min. The supernatant was then decanted into another furnaced culture tube (II) and 2 mL of dichloromethane extracted double distilled water was added. In order to recover any lipids not fully solubilised by the methanol solution, 2 × 3 mL of *n*−hexane was added to the extracted potsherds contained in the original culture tubes, mixed well and transferred to culture tube II. The extraction was transferred to a clean, furnaced 3.5 mL vial and blown down to dryness. Following this, 2 × 2 mL *n*−hexane was added directly to the H_2SO_4/MeOH solution in culture tube II and whirlimixed to extract the remaining residues. This was transferred to the 3.5 mL vials and blown down under a gentle stream of nitrogen until a full vial of *n*−hexane remained. Aliquots of the extracts (containing fatty acid methyl esters, FAME's) were derivatised using *N,O*−bis(trimethylsilyl)trifluoroacetamide (BSTFA) containing 1% *v/v* trimethylchlorosilane (TMCS; Sigma Aldrich Company Ltd.; 20μL; 70°C,

1h). Excess BSTFA was removed under nitrogen and the extract was dissolved in *n*−hexane for analysis by gas chromatography (GC), GC–mass spectrometry (GC–MS) and GC–combustion–isotope ratio MS (GC–C–IRMS).

Firstly, the samples underwent gas chromatography using a gas chromatograph (GC) fitted with a high temperature non−polar column (DB1−HT; 100% dimethylpolysiloxane, 15m × 0.32mm i.d., 0.1μm film thickness). The carrier gas was helium and the temperature programme comprised a 50°C isothermal hold followed by an increase to 350°C at a rate of 10°C min^{-1} followed by a 10 min isothermal hold. A procedural blank (no sample) was prepared and analysed alongside every batch of samples. Further compound identification was accomplished using gas chromatography−mass spectrometry (GC−MS). FAMEs were introduced by autosampler onto a GC−MS fitted with a non−polar column, 50m × 0.32mm fused silica capillary column coated with an Rtx−1 stationary phase (100% dimethylpolysiloxane, Restek, 0.17μm). The instrument was a ThermoScientific Trace 1300 gas chromatograph coupled to an ISQ single quadrupole mass spectrometer. Samples were run in full scan mode (*m/z* 50–650) and the temperature programme comprised an isothermal hold at 50°C for 1 min, followed by a gradient increase to 300°C at 10°C min^{-1}, followed by an isothermal hold at 300°C (15 min). The MS was operated in electron ionisation (EI) mode operating at 70 eV. Data acquisition and processing were carried out using the HP Chemstation software (Rev. C.01.07 (27), Agilent Technologies) and Xcalibur software (version 3.0). Peaks were identified on the basis of their mass spectra and GC retention times, by comparison with the NIST mass spectral library (version 2.0).

Carbon isotope analyses by GC−C−IRMS were also carried out using a GC Agilent Technologies 7890A coupled to an Isoprime 100 (EI, 70eV, three Faraday cup collectors *m/z* 44, 45 and 46) via an IsoprimeGC5 combustion interface with a CuO and silver wool reactor maintained at 850°C. Instrument accuracy was determined using an external FAME standard mixture (C_{11}, C_{13}, C_{16}, C_{21} and C_{23}) of known isotopic composition. Samples were run in duplicate and an average taken. The $\delta^{13}C$ values are the ratios $^{13}C/^{12}C$ and expressed relative to the Vienna Pee Dee Belemnite, calibrated against a CO_2 reference gas of known isotopic composition. Instrument error was ±0.3‰. Data processing was carried out using Ion Vantage software (version 1.6.1.0, IsoPrime).

4. Phytolith analysis: materials and methods

4.1 Technology and function of grinding tools

Petrographic features, manufacture and use−wear traces were investigated using well−established methods (for a general overview, see Delgado−Raack 2008: 188–226; Adams *et al.* 2009; Dubreuil *et al.* 2015). Following procedures applied in field petrography, a lithological determination of the artefacts (Table S8) was conducted at the macro and low−power microscopic levels (up to 40×), using the terminology for coarse and heterogeneous rocks. With the aim of defining their carbonatic or silificed nature, a 0.8M hydrochloric acid dilution was applied to carefully selected areas of the artefacts. Geomorphological criteria including comparison between naturally rolled and anthropically abraded surfaces as well as metrical proportions were used to discern between cobbles and quarried rock pieces (Risch 2002).

Table S8: Summary of the main technological features related to lithic artefacts. Abrader: tool of small dimensions (normally thin and not longer than 100mm) involved in frictional tasks. Handstone: active part of a grinding equipment reciprocally acting with a grinding slab; grinding slab: passive part of a grinding equipment; stone slab: stone block used as a passive platform, on which several tasks involving friction and percussion were performed; light container: stone artefact that shows a burned concavity on its obverse as a consequence of having contained burning fuel; percussor: tool used for striking against another material.

Inv. number	Type of artefact	Lithology	Manufacturing evidence (number of surfaces)	Use evidence (number of surfaces)	Recycling evidence
116/17	Abrader-percussor	Silicified conglomerate	0	4	
158/18	Handstone	Silicified sandstone	3	1	X
159/18	Stone slab	Silicified sandstone	2	3	
160/18	Handstone?	Silicified sandstone	1	2	
161/18	Undetermined	Silicified sandstone	1	1	
	(Light container?)				
162/18	Grinding slab?	Silicified sandstone	1	1	
163/18	Abrader/ handstone?	Silicified sandstone	2	1	
164/17	Undetermined	Undetermined	0	0	
164/18	Abrader	Silicified sandstone	5	1	
166/18	Stone slab	Calcarenite	0	1	
171/56	Handstone	Silicified sandstone	3	2?	X

To determine artefact use, the morphology, size and weight of each fragment were recorded (Hürlimann 1965; Zimmermann 1988; Delgado−Raack & Risch 2016), as well as evidence of manufacture (e.g. knapping for primary shaping of the artefact, pecking to regularise surfaces or create a rough texture, and abraded edges to delete abrupt angles) (Risch 2002; Delgado-Raack 2008). Qualitative parameters to identify wear traces, including levelling, striations, pits, hand polish, grain extraction, grain fractures or grain rounding were examined macroscopically and using low power microscopy (up to 63×) using a stereo microscope (OlympusSZ−STU1; Dubreuil 2002; Hamon 2006; Delgado-Raack 2008; Adams *et al.* 2009). Finally, the interpretation of use−wear and tool kinetics is based on comparative analysis from several experimental programs developed to evaluate the most likely uses as well as the processed materials (Adams *et al.* 2009: appendix 2; Dubreuil *et al.* 2015: tab. 7.7).

4.2 Phytolith analysis from macrolithic stone tools

The methods used are similar to those developed by Katz *et al.* (2010). A weighed aliquot of between 30–40mg of dried sediment was treated with 50µl of a volume solution of 6N HCl. Aliquots of 50µl of material were mounted on microscope slides using 24 × 24 cover slips. Phytoliths were examined in random fields at 200× and 400× magnification using an Olympus Bx43 optical microscope. A minimum of 200 phytoliths with diagnostic morphologies were counted. The estimated phytolith numbers per gram of sediment were related to the initial sample weight and allow quantitative comparisons between the samples. Phytoliths that were unidentifiable because of dissolution were recorded as weathered morphotypes. Morphological identification was based on modern plant reference collections and standard literature (Twiss *et al.* 1969; Brown 1984; Mulholland & Rapp 199; 2Rosen 1992; Twiss 1992; Albert & Weiner 2001; Piperno 2006; Tsartsidou *et al.* 2007; Albert *et al.* 2008, 2016; Portillo *et al.* 2014). The terms used to describe phytolith morphologies follow the standards of the International Code for Phytolith Nomenclature-ICPN 2.0 (Neumann *et al.* 2019).

4.3 Phytolith and residue microscopic analyses from dental calculus

Dental calculus samples were suspended in ~1.5 ml of 0.6 M HCl. After 15 min, the samples were centrifuged at room temperature at 10 000 rpm for 5 min and the pellet washed in distilled water. Sample material was transferred onto microscope slides, in 50% glycerol in distilled water. Several slides were mounted and examined from each sample. Microscopic analysis was conducted on an Olympus IX 71 inverted microscope using magnifications between 50× and 200×. Digital images were obtained using a Colour View camera from Olympus and Cell D imaging system. Phytoliths and all visible material were recorded (Table S9).

Table S9. Description, provenance of samples and main phytolith results from Khor Shambat samples.

Sample number	Phytoliths 1g of sediment (million)	Number of phytoliths counted	% Phytoliths weathering	% Multicelled phytoliths	% Grass phytoliths	Description/ sample type
116/17	3.01	228	2.6	0	93.8	Abrader−percussor
158/18	0.44	110	11.8	0.9	78	Handstone
159/18	0.07	22	11.1	0	82.2	Stone slab
160/18	0.71	216	2.3	1.9	88.4	Handstone?

161/18	0.13	230	21.2	0	77.6	Undetermined
162/18	0.08	23	14.4	0	68.7	Grinding slab?
163/18	0.23	79	13.9	0	78.5	Abrader/handstone?
164/17	4.40	262	5.3	2.7	89.8	Undetermined
164/18	0.43	110	14.6	0	77.8	Abrader
166/18	3.40	241	5.4	2.1	88.9	Stone slab
171/56	0.08	23	9.1	9.1	78.2	Handstone
Level 145−150m	0.42	122	13.9	3.3	71	Sediment sample,
Grave 51/ Pottery 3	0.78	234	8.5	4.3	83.4	Sediment sample
Grave 14−1		9				Dental calculus, teeth 1
Grave 14−2		12				Dental calculus, teeth 2
Grave 15		2				Dental calculus
Grave 51		2				Dental calculus
Grave 63		5				Dental calculus

Phytoliths were observed in all the calculus samples. Phytolith assemblages were dominated again by grasses, including in characteristic morphotypes from both the leaves and stems (prickles, bulliform cells, multicelled psilate long cells), as well as the inflorescences (epidermal appendage hair form the awn). Interestingly, both samples from Grave 14 yielded a single diagnostic short cell bilobate from Panicoids (samples 14−1 and 14−2; Figure S2h). Additionally, dicotyledoneous phytoliths such as epidermal appendages, and spheroid were also noted (Figure S2i). Regarding preservation conditions, it should be noted that only one multicelled phytolith was observed (sample 51), and that certain morphotypes were unidentifiable due to deformations by chemical dissolution (weathered) or high temperatures (melted) (Figure S2j−k). Of particular note is the identification of partially melted phytoliths in association to fragments of micro−charcoal and charred organic pieces (samples 14−1 and 15; Figure S2l), therefore pointing to the consumption of burned/cooked plant−foods. As previously argued, none of the calculus assemblages displayed starch granules. Pollen grains, fungal spores or insect remains were not observed either. However, long fibers, presumably of plant origin, were observed in all the samples, together with mineral aggregates.

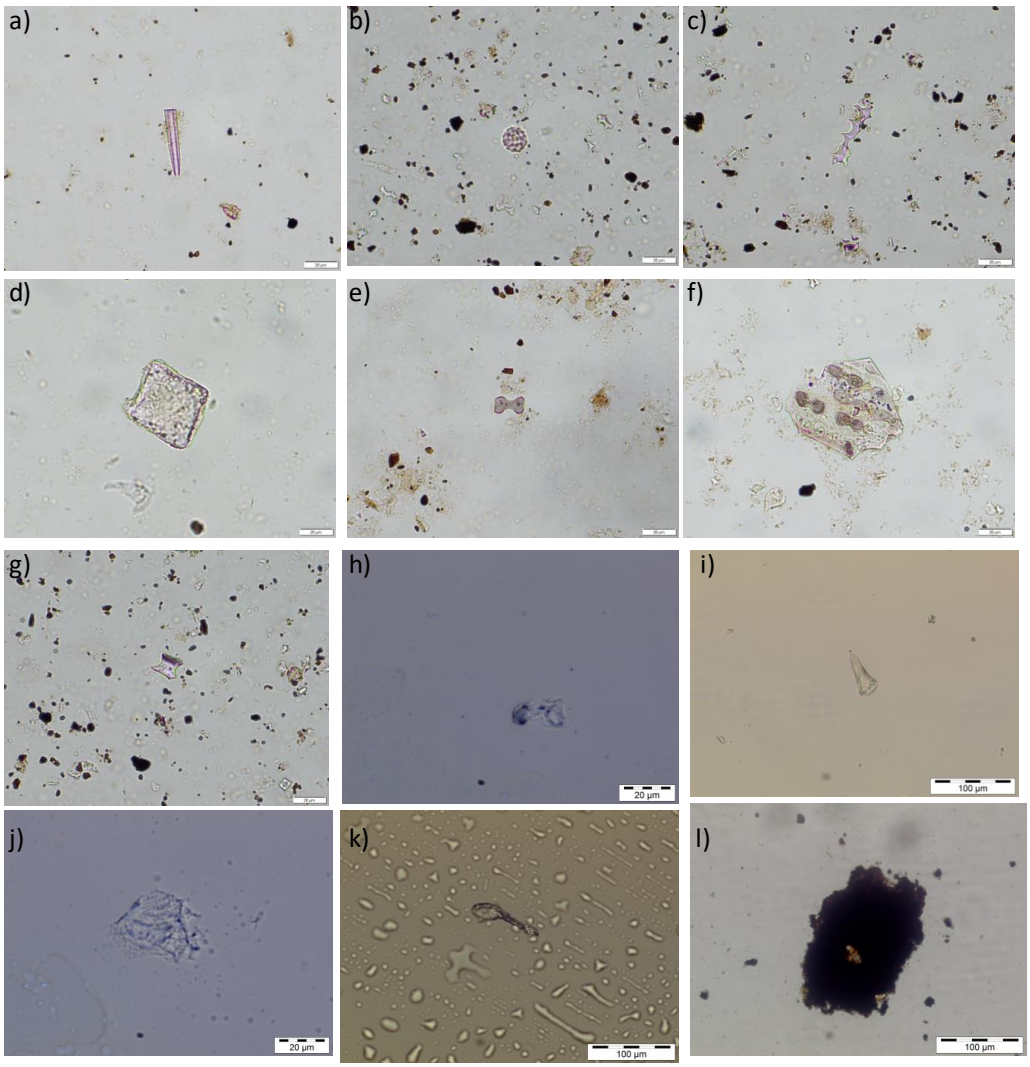

Figure S2. Photomicrographs of phytoliths and other micro−remains identified in Khor Shambat samples (photographs taken at 400× or 200×): a) Sponge spicule, sample 164/18; b) spheroid echinate from palm (Arecaceae) leaves, 166/18; c) long cell dendritic from grass inflorescences, 166/18; d) bulliform cell, 163/18; e) short cell bilobate from Panicoideae grasses, 158/18; f) multicelled phytoliths from Panicoideae, 16/17; g) short cell rondel from Pooideae grasses, 166/18; h) short cell bilobate from Panicoideae (partially weathered), 15; i) epidermal appendage hair from dicotyledoneous, 15; j) weathered phytolith (possibly bulliform cell), 44; k) partially melted single cell (likely bilobate), 14−1; l) micro−charcoal, 15 (micrographs by M. Portillo).

5. Comparative analysis: faunal remains and organic residues

Comparison of two independent datasets on animal exploitation strategies, the pottery lipid residues and faunal remains, can provide greater insight into the nature of faunal exploitation at Khor Shambat (e.g. Dunne *et al.* 2019). Our data, however, has high levels of uncertainty

on two fronts; 1) sample sizes and 2) the likelihood of domestic ruminants being bred for meat or dairy. We therefore need to incorporate these uncertainties into our data representation (see above: Material and Methods). The first is sample size and is common to both the faunal data and lipid profiles. The lipid recovery rate was fairly low, and therefore the number of sherds with each of the fat types is only a small sample of what would have originally been processed in those pots. Such small sample size introduces a large uncertainty margin when estimating proportions. The second level of uncertainty regards only the faunal data, specifically the domestic ruminant remains. Whilst the lipid profiles distinguish between ruminant adipose and dairy fats, we cannot say with any certainty whether the domestic ruminants in the faunal remains were bred primarily for meat or milk. To accommodate the uncertainty introduced from small sample size we use the NISP counts and number of fat types and randomly sample those numbers from a Dirichlet distribution. This allows us to put an error margin on the proportions of different fat types (Figure 9). This is relatively straightforward for the Mesolithic phase due to the absence of any domestic taxa. For the Neolithic, however, we also need to consider whether the domestic faunal remains represent animals bred for dairy products or meat. Because the age profile for the cattle and small ruminants suggests that they were bred mostly for their secondary products, we apply a prior estimate of 75 per cent of all domestic ruminant remains being used for dairy, which we sample, this time from a beta distribution, to represent the uncertainty. This is only an estimate, and the proportion of bones representing dairy can be changed according to any new prior beliefs (see Figures 9 & 10).

References

ADAMS, J. *et al.* 2009. Functional analysis of macro−lithic artefacts: a focus on working surfaces, in F. Sternke, L. Eigeland & L.J. Costa (ed.) *L'utilisation préhistorique de matières premières lithiques alternatives* (British Archaeological Reports International Series 1939): 43–66. Oxford: Archaeopress.

ALBERT, R.M. & S. WEINER. 2001. Study of phytoliths in prehistoric ash layers from Kebara and Tabun caves using a quantitative approach, in J.D. Meunier & F. Colin (ed.) *Phytoliths: applications in Earth Sciences and Human History*: 251–66. Lisse: Balkema. https://doi.org/10.1201/NOE9058093455.ch19

ALBERT, R.M., J.A. RUIZ & A. SANS. 2016. PhytCore ODB: a new tool to improve efficiency in the management and exchange of information on phytoliths. *Journal of Archaeological Science* 68: 98–105. https://doi.org/10.1016/j.jas.2015.10.014

ALBERT, R.M. *et al.* 2008. Phytolith–rich layers from the Late Bronze and Iron Ages at Tel Dor (Israel): mode of formation and archaeological significance. *Journal of Archaeological Science* 35: 57–75. https://doi.org/10.1016/j.jas.2007.02.015

BELDADOS, A. 2015. *Paleoethnobotanical study of ancient food crops and the environmental context in North East Africa, 6000 BC–200/300 AD* (British Archaeological Reports International Series 2706). Oxford: Archaeopress. https://doi.org/10.30861/9781407313573

– 2017. Archaeobotanical investigation of charred and desiccated fruit stones and seeds from Late Holocene contexts in Kassala and its environs: window to past ecology and subsistence. *Ethiopian Journal of the Social Sciences and Humanities* 13. https://doi.org/10.4314/ejossah.v13i1

BROWN, D.A. 1984. Prospects and limits of a phytolith key for grasses in the central United States. *Journal of Archaeological Science* 11: 345–68. https://doi.org/10.1016/0305–4403(84)90016–5

CORREA–ASCENCIO, M. & R.P. EVERSHED. 2014. High throughput screening of organic residues in archaeological potsherds using direct acidified methanol extraction. *Analytical Methods* 6: 1330–40. https://doi.org/10.1039/c3ay41678j

DELGADO–RAACK, S. 2008. *Prácticas económicas y gestión social de recursos (macro)líticos en la prehistoria reciente (III–I milenios ac) del Mediterráneo occidental*. Bellaterra: Universitat Autònoma de Barcelona. Available at: https://ddd.uab.cat/pub/tesis/2008/tdx–0212109–094347/sdr1de2.pdf (accessed 20 March 2020).

DELGADO–RAACK, S. & R. RISCH. 2016. Bronze Age cereal processing in Southern Iberia: a material approach to the production and use of grinding equipment. *Journal of Lithic Studies* 3: 125–45. https://doi.org/10.2218/jls.v3i3.1650

DUBREUIL, L. 2002. Étude fonctionnelle des outils de broyage natoufiens: nouvelles perspectives sur l'émergence de l'agriculture au Proche–Orient. Unpublished PhD dissertation, Université Bordeaux I.

DUBREUIL, L. *et al.* 2015. Current analytical frameworks for studies of use–wear on ground stone tools, in J.M. Marreiros, J.F. Gibaja Bao & N. Ferreira Bicho (ed.) *Use–wear and residue analysis in archaeology. Manuals in archaeological method, theory and technique*: 105–58. New York: Springer. https://doi.org/10.1007/978–3–319–08257–8_7

DUDD, S.N. & R.P. EVERSHED. 1998. Direct demonstration of milk as an element of archaeological economies. *Science* 282: 1478–81. https://doi.org/10.1126/science.282.5393.1478

DUNNE, J. *et al*. 2019. Pots, plants and animals: broad−spectrum subsistence strategies in the Early Neolithic of the Moroccan Rif region. *Quaternary International* 555: 96–109. https://doi.org/10.1016/j.quaint.2019.12.009

EVERSHED, R.P. 2008. Experimental approaches to the interpretation of absorbed organic residues in archaeological ceramics. *World Archaeology* 40: 26–47. https://doi.org/10.1080/00438240801889373

EVERSHED, R.P. *et al*. 1997. New criteria for the identification of animal fats preserved in archaeological pottery. *Naturwissenschaften* 84(9): 402–406. https://doi.org/10.1007/s001140050417

– 2002. Chemistry of archaeological animal fats. *Accounts of Chemical Research* 35: 660–8. https://doi.org/10.1021/ar000200f

HAMON, C. 2006. *Broyage et abrasion au Néolithique ancient: caractérisation technique et fonctionnelle des outillages en grès du Bassin parisien* (British Archaeological Reports International Series 1551). Oxford: Archaeopress. https://doi.org/10.30861/9781841719801

HÜRLIMANN, F. 1965. Neolithische Reibmühlen von einer Ufersiedlung am Greifensee. *Jahrbuch der Schweizerischen Gesellschaft für Urgeschichte* 52: 72–86.

KATZ, O. *et al*. 2010. Rapid phytolith extraction for analysis of phytolith concentrations and assemblages during an excavation: an application at Tell es−Safi/Gath, Israel. *Journal of Archaeological Science* 37: 1557–63. https://doi.org/10.1016/j.jas.2010.01.016

KUBIAK−MARTENS, L. 2011. Botanical evidence, in M. Chłodnicki, M. Kobusiewicz & K. Kroeper (ed.) *Kadero*: *the Lech Krzyzaniak excavations in the Sudan*: 409–15. Poznan: PAM.

MAJID, A. 1989. Exploitation of plants in the Eastern Sahel (Sudan), 5000–2000 BC, in L. Krzyżaniak & M. Kobusiewicz (ed.) *Late prehistory of the Nile Basin and the Sahara*: 459–68. Poznan: PAM.

MARGUERIE D. & J.−Y. HUNOT. 2007. Charcoal analysis and dendrology: data from archaeological sites in north−western France. *Journal of Archaeological Science* 34: 1417–33. https://doi.org/10.1016/j.jas.2006.10.032

MOSKAL−DEL HOYO, M., M. WACHOWIAK & R.A. BLANCHETTE. 2010. Preservation of fungi in charcoal. *Journal of Archaeological Science* 37: 2106–16. https://doi.org/10.1016/j.jas.2010.02.007

MULHOLLAND, S.C. & G. RAPP. 1992. A morphological classification of grass silicabodies, in G. Rapp & S.C. Mulholland (ed.) *Phytolith systematics: emerging issues, advances in archaeological and museum science*: 65–89. New York: Plenum. https://doi.org/10.1007/978−1−4899−1155−1_4

NEUMANN, K., W. SCHOCH, P. DETIENNE & F.H. SCHWEINGRUBER. 2001. *Woods of the Sahara and the Sahel: an anatomical atlas*. Bern: Paul Haupt.

NEUMANN, K. *et al.* 2019. International Code for Phytolith Nomenclature (ICPN) 2.0. *Annals of Botany* 124: 189–99. https://doi.org/10.1093/aob/mcz064

PETERS, J. 1986. *Osteomorphology and osteometry of the appendicular skeleton of Grant's gazelle, Gazella Granti Brooke, 1871, Bohor reedbuck*, Redunca redunca *(Pallas 1767) and Bushbuck, Tragelaphus scripts (Pallas, 1766)*. Ghent: Rijksuniversiteit.

– 1989a. Osteomorphological features of the appendicular skeleton of gazelles, genus Gazella Blainville 1816, Bohor Reedbuck. *Tragelaphus scriptus* (Pallas, 1766). *Anatomia, Histologia, Embryologia* 18: 97–192. https://doi.org/10.1111/j.1439−0264.1989.tb00586.x

– 1989b. *Faunal remains and environmental change in Central and Eastern Sudan from terminal Pleistocene to Middle Holocene times* (Mededelingen van de Koninlijke Academie voor Wetenschappen, Letteren en Schone Kunsten van België, Klasse der Wetenschappen, Jaargang 51, Nr 4). Brussels: Koninklijke academie voor wetenschappen, letteren en schone kunsten van België.

PETERS, J., W. VAN NEER & I. PLUG. 1997. *Comparative postcranial osteology of Hartbeest (*Alcelaphus buselaphus*), Scimitar oryx (*Oryx dammah*) and Addax (*Addax nasomaculatus*), with notes on the osteometry of gemsbok (*Oryx gazelle*) and Arabian oryx (*Oryx leucoryx*)* (Annales Sciences Zoologiques 280). Tervuren: Musee Royal de L'Afrique Centrale.

PIPERNO, D.R. 2006. *Phytoliths: a comprehensive guide for archaeologists and paleoecologists*. Lanham (MD): Altamira.

PLUG, I. 2014. What bone is that? A guide to the identification of southern African mammal bones. Pretoria: STN.

PORTILLO, M., S. KADOWAKI, Y. NISHIAKI & R.M. ALBERT. 2014. Early Neolithic household behavior at Tell Seker al−Aheimar (Upper Khabur, Syria): a comparison to ethnoarchaeological study of phytoliths and dung spherulites. *Journal of Archaeological Science* 42: 107–18. https://doi.org/10.1016/j.jas.2013.10.038

RISCH, R. 2002. *Recursos naturales, medios de producción y explotación social: un análisis económico de la industria lítica de Fuente Alamo (Almería), 2250–1400 ANE*. Manheim: Philipp von Zabern.

ROSEN, A.M. 1992. Preliminary identification of silica skeletons from Near Eastern archaeological sites: an anatomical approach, in G. Rapp & S.C. Mulholland (ed.) *Phytolith systematics: emerging issues, advances in archaeological and museum science:* 129–48. New York: Plenum. https://doi.org/10.1007/978−1−4899−1155−1_7

TSARTSIDOU, G. *et al.* 2007. The phytolith archaeological record: strengths and weaknesses evaluated based on a quantitative modern reference collection from Greece. *Journal of Archaeological Science* 34: 1262–75. https://doi.org/10.1016/j.jas.2006.10.017

TWISS, P.C. 1992. Predicted world distribution of C_3 and C_4 grass phytolith, in G. Rapp & S.C. Mulholland (ed.) *Phytolith systematics: emerging issues, advances in archaeological and museum science:* 113–28. New York: Plenum.

TWISS, P.C., E. SUESS & R.M. SMITH. 1969. Morphological classification of grass phytoliths. *Soil Science Society of America Proceedings* 33: 109–15. https://doi.org/10.1007/978−1−4899−1155−1_6

VAN NEER, W. 1989. *Contribution to the archaeozoology of Central Africa* (Annales Sciences Zoologiques 259). Tervuren: Musee Royal de L'Afrique Centrale.

– 2004. Evolution of prehistoric fishing in the Nile Valley. *Journal of African Archaeology* 2: 251–26. https://doi.org/10.3213/1612−1651−10030

VON DEN DRIESCH, A. 1976. *A guide to the measurement of animal bones from archaeological sites* (Peabody Museum Bulletin 1). Cambridge (MA): Peabody Museum.

WALKER, R. 1985. *A guide to post−cranial bones of East African animals*. Norwich: Hylochoerus.

ZIMMERMANN, A. 1988. Steine, in U. Böelicke *et al.* (ed.) *Der bandkeramische Fundplatz Langweiler 8, Gemeinde Aldenhoven, Kr. Düren, Beiträge zur neolithischen Besiedlung der Aldenhovener Platte III* (Rheinische Ausgrabungen 28): 569–787. Cologne: Rheinland.